UNIVERSIDAD DE CONCEPCIÓN

Centro de Investigación en Ingeniería Matemática (CI^{2}MA)

A momentum and mass conservative pseudostress-based mixed finite element method for the Stokes problem

Jessika Camaño, Ricardo Oyarzúa,
Katherine Rojo

PREPRINT 2025-06

SERIE DE PRE-PUBLICACIONES

A momentum and mass conservative pseudostress-based mixed finite element method for the Stokes problem *

Jessika Camaño† Ricardo Oyarzúa‡ Katherine Rojo§

Abstract

In this paper, we analyze a pseudostress-based mixed finite element method for the Stokes problem that ensures both mass and momentum conservation. Mass conservation is achieved by approximating the velocity using the lowest-order Raviart–Thomas elements, while momentum conservation is enforced through a discrete Helmholtz decomposition of the piecewise-constant vector space. We establish the well-posedness of the method and derive theoretical convergence rates, including a superconvergence result for the velocity gradient approximation. A key advantage of the proposed method is its computational efficiency, as it is slightly less expensive than the classical pseudostress-based approach studied in [5, 11], while also guaranteeing mass and momentum conservation. Additionally, we extend our analysis to the Stokes problem with mixed boundary conditions and present numerical experiments that confirm the theoretical results.

Key words: Stokes problem; pseudostress; mass and momentum conservation; divergence-free velocities, Helmholtz descomposition

1 Introduction

In this paper, we propose and analyze a mass- and momentum-conservative numerical scheme for a pseudostress-based formulation of the Stokes problem.

To provide more details on our approach, we begin by recalling the classical Stokes problem, governed by the following system of partial differential equations:

$$-\nu\Delta\mathbf{u} + \nabla p = \mathbf{f} \quad \text{in } \Omega, \quad \operatorname{div}\mathbf{u} = 0 \quad \text{in } \Omega, \quad \mathbf{u} = \mathbf{u}_D \quad \text{on } \Gamma, \quad \int_\Omega p = 0. \tag{1.1}$$

*This research was partially supported by ANID-Chile through projects Fondecyt Regular 1231336, Centro de Modelamiento Matemático (FB210005) and Anillo of Computational Mathematics for Desalination Processes (ACT210087), and by DI-UCSC through the project FGII 06/2024.

†GIANuC^2-Departamento de Matemática y Física Aplicadas, Universidad Católica de la Santísima Concepción, Casilla 297, Concepción, Chile, and CI^{2}MA, Universidad de Concepción, Casilla 160-C, Concepción, Chile, email: jecamano@ucsc.cl

‡GIMNAP-Departamento de Matemática, Universidad del Bío-Bío, Casilla 5-C, Concepción, Chile, and CI^{2}MA, Universidad de Concepción, Casilla 160-C, Concepción, Chile, email: royarzua@ubiobio.cl

§GIANuC^2-Departamento de Matemática y Física Aplicadas, Universidad Católica de la Santísima Concepción, Concepción, Chile, email: krojo@magister.ucsc.cl

This system describes the motion of an incompressible fluid with velocity $\mathbf{u} = (u_1, \ldots, u_d)^t$, pressure p, and viscosity $\nu > 0$ in a region $\Omega \subseteq \mathbb{R}^d$ $(d = 2, 3)$, subjected to a source force $\mathbf{f} = (f_1, \ldots, f_d)^t$ and a prescribed velocity $\mathbf{u}_D = (u_{D,1}, \ldots, u_{D,d})^t$ on the boundary $\Gamma := \partial\Omega$, satisfying the compatibility condition:

$$\int_\Gamma \mathbf{u}_D \cdot \mathbf{n} = 0. \tag{1.2}$$

Here, $\mathbf{n} = (n_1, \ldots, n_d)^t$ denotes the outward unit normal vector on Γ.

In [5] and [11] (see also [10] for a similar approach), the so-called pseudostress tensor given by:

$$\boldsymbol{\sigma} := \nu\nabla\mathbf{u} - p\,\mathbb{I} \quad \text{in } \Omega, \tag{1.3}$$

is introduced to reformulate (1.1) as follows:

$$\boldsymbol{\sigma}^{\mathrm{d}} = \nu\nabla\mathbf{u} \quad \text{in } \Omega, \quad -\mathbf{div}\,\boldsymbol{\sigma} = \mathbf{f} \quad \text{in } \Omega, \quad \mathbf{u} = \mathbf{u}_D \quad \text{on } \Gamma, \quad \int_\Omega \mathrm{tr}\,(\boldsymbol{\sigma}) = 0, \tag{1.4}$$

where $\mathbb{I}$ denotes the identity matrix, $\mathrm{tr}\,(\boldsymbol{\sigma})$ is the trace of the tensor $\boldsymbol{\sigma}$, $\boldsymbol{\sigma}^{\mathrm{d}} := \boldsymbol{\sigma} - \frac{1}{d}\mathrm{tr}\,(\boldsymbol{\sigma})\mathbb{I}$ denotes the deviatoric part of $\boldsymbol{\sigma}$, and $\mathbf{div}\,\boldsymbol{\tau}$ is the divergence operator div acting along the rows of $\boldsymbol{\tau}$ for any tensor field $\boldsymbol{\tau} = (\tau_{ij})_{i,j=1,d}$.

Based on (1.4), the works [5] and [11] study conforming numerical discretizations for the following variational problem: Find $\boldsymbol{\sigma} \in \mathbb{H}_0(\mathbf{div}\,;\Omega)$ and $\mathbf{u} \in \mathbf{L}^2(\Omega) = [\mathrm{L}^2(\Omega)]^d$ such that

$$\begin{aligned} \frac{1}{\nu}(\boldsymbol{\sigma}^{\mathrm{d}}, \boldsymbol{\tau}^{\mathrm{d}})_\Omega + (\mathbf{u}, \mathbf{div}\,\boldsymbol{\tau})_\Omega &= \langle \boldsymbol{\tau}\mathbf{n}, \mathbf{u}_D\rangle_\Gamma\,, \quad \forall \boldsymbol{\tau} \in \mathbb{H}_0(\mathbf{div}\,;\Omega), \\ (\mathbf{v}, \mathbf{div}\,\boldsymbol{\sigma})_\Omega &= -(\mathbf{f}, \mathbf{v})_\Omega, \qquad \forall \mathbf{v} \in \mathbf{L}^2(\Omega), \end{aligned} \tag{1.5}$$

where, for simplicity, we use the following notation:

$$(v, w)_\Omega := \int_\Omega vw, \quad (\mathbf{v}, \mathbf{w})_\Omega := \int_\Omega \mathbf{v}\cdot\mathbf{w}, \quad (\boldsymbol{\tau}, \boldsymbol{\zeta})_\Omega := \sum_{i,j=1}^{d} \int_\Omega \tau_{ij}\zeta_{ij},$$

for any scalars v, w, vectors $\mathbf{v} = (v_i)_{i=1,d}$, $\mathbf{w} = (w_i)_{i=1,d}$, and tensor fields $\boldsymbol{\zeta} = (\zeta_{ij})_{i,j=1,n}$, $\boldsymbol{\tau} = (\tau_{ij})_{i,j=1,n}$. In addition, $\langle\cdot,\cdot\rangle_\Gamma$ denotes the duality pairing between the trace space $\mathrm{H}^{1/2}(\Gamma)$ and its dual $\mathrm{H}^{-1/2}(\Gamma)$, which coincides with the $\mathrm{L}^2(\Gamma)$-inner product when applied to functions in $\mathrm{L}^2(\Gamma)$.

Here, $\mathbb{H}(\mathbf{div}\,;\Omega)$ denotes the space of tensors whose rows belong to

$$\mathbf{H}(\mathrm{div};\Omega) := \{\mathbf{v} \in \mathbf{L}^2(\Omega) : \mathrm{div}\,\mathbf{v} \in \mathrm{L}^2(\Omega)\},$$

and $\mathbb{H}_0(\mathbf{div}\,;\Omega)$ is the subspace of $\mathbb{H}(\mathbf{div}\,;\Omega)$ given by

$$\mathbb{H}_0(\mathbf{div}\,;\Omega) := \{\boldsymbol{\tau} \in \mathbb{H}(\mathbf{div}\,;\Omega) : (\mathrm{tr}\,(\boldsymbol{\tau}), 1)_\Omega = 0\}.$$

In [5] and [11], it is shown that selecting Raviart–Thomas elements of degree $k \geq 0$ or Brezzi–Douglas–Marini (BDM) elements of order $k+1$ for $\mathbb{H}(\mathbf{div}\,;\Omega)$ and piecewise polynomials of degree k for $\mathbf{L}^2(\Omega)$ leads to a well-posed and optimally convergent conforming discretization of (1.5). In addition, from the second equation of (1.5) it can be seen that the equilibrium

equation $\mathbf{div}\,\boldsymbol{\sigma} = -\mathbf{f}$ is exactly satisfied if $\mathbf{f}$ belongs to the same discrete space as the velocity. Consequently, the method preserves momentum. However, since the condition $\operatorname{div}\mathbf{u} = 0$ in Ω cannot be ensured at the discrete level, the method lacks mass conservation (see Example 4 in Section 5). To overcome this the lack of mass conservation, in [6] is introduced the following variational formulation based on (1.4): Find $\boldsymbol{\sigma} \in \mathbb{H}_0(\mathbf{div}\,;\Omega)$, $\mathbf{u} \in \mathbf{H}(\operatorname{div}^0;\Omega)$ and $\varphi \in \mathrm{H}^1_0(\Omega)$, such that

$$\begin{aligned} \frac{1}{\nu}(\boldsymbol{\sigma}^{\mathrm{d}},\boldsymbol{\tau}^{\mathrm{d}})_\Omega + \frac{1}{\nu}(\mathbf{div}\,\boldsymbol{\sigma},\mathbf{div}\,\boldsymbol{\tau})_\Omega + (\mathbf{u}+\nabla\varphi,\mathbf{div}\,\boldsymbol{\tau})_\Omega &= \langle \boldsymbol{\tau}\mathbf{n},\mathbf{u}_D\rangle_\Gamma - \frac{1}{\nu}(\mathbf{f},\mathbf{div}\,\boldsymbol{\tau})_\Omega, \\ (\mathbf{v}+\nabla\psi,\mathbf{div}\,\boldsymbol{\sigma})_\Omega &= -(\mathbf{f},\mathbf{v}+\nabla\psi)_\Omega, \end{aligned} \tag{1.6}$$

for all $\boldsymbol{\tau} \in \mathbb{H}_0(\mathbf{div}\,;\Omega)$ and $(\mathbf{v},\psi) \in \mathbf{H}(\operatorname{div}^0;\Omega)\times \mathrm{H}^1_0(\Omega)$, where

$$\mathrm{H}^1_0(\Omega) := \{\psi \in \mathrm{H}^1(\Omega) : \psi = 0 \text{ on } \Gamma\} \quad \text{and} \quad \mathbf{H}(\operatorname{div}^0;\Omega) := \{\mathbf{v} \in \mathbf{H}(\operatorname{div};\Omega) : \operatorname{div}\mathbf{v} = 0 \text{ in } \Omega\}.$$

In [6], it is proven that $\varphi = 0$ in Ω and consequently, problems (1.6) and (1.5) are equivalent, with the key argument relying on the Helmholtz decomposition:

$$\mathbf{L}^2(\Omega) = \mathbf{H}(\operatorname{div}^0;\Omega) \oplus \mathrm{H}^1_0(\Omega).$$

Furthermore, by selecting Raviart–Thomas elements of degree $k \geq 0$ or BDM elements of degree $k+1$ for the tensor $\boldsymbol{\sigma}$, Raviart–Thomas elements of degree k for the velocity $\mathbf{u}$, and continuous piecewise polynomials of degree $k+1$ for $\mathrm{H}^1_0(\Omega)$, it is shown that the resulting conforming Galerkin discretization is well-posed, optimally convergent, and mass-conservative. However, the approach proposed in [6] fails to ensure momentum conservation. This is because the equation

$$(\mathbf{v}+\nabla\psi,\mathbf{div}\,\boldsymbol{\sigma}+\mathbf{f})_\Omega = 0, \tag{1.7}$$

for all discrete functions $\mathbf{v}$ and ψ in their respective discrete spaces does not necessarily imply that the equilibrium equation $\mathbf{div}\,\boldsymbol{\sigma} = -\mathbf{f}$ is exactly satisfied in Ω, even when $\mathbf{f}$ is approximated by piecewise polynomials.

Building on the above discussion and aiming to contribute to the development of numerical schemes for fluid flow problems that preserve conservation laws, we propose a new pseudostress-based numerical scheme that exactly preserves mass and momentum, where the latter holds for $\mathbf{f}$ in a suitably chosen piecewise polynomial space.

To achieve this, we discretize an equivalent reduced version of the three-field variational formulation (1.6), employing BDM elements of order 1 or Raviart–Thomas elements of order 0 for $\boldsymbol{\sigma}$ and $\boldsymbol{\tau}$, Raviart–Thomas elements of order 0 for $\mathbf{u}$ and $\mathbf{v}$, and the lowest-order Crouzeix–Raviart element (see [7]) for φ and ψ.

The key argument for ensuring momentum conservation is the discrete Helmholtz decomposition of piecewise constant functions into divergence-free Raviart–Thomas elements of order zero and gradients of Crouzeix–Raviart elements, as established in [2] (see also [17]). The above allows us to conclude from (1.7) that the momentum equation is exactly satisfied in Ω if $\mathbf{f}$ is piecewise constant.

It is important to note that, in this approach, as well as in the previous works [5], [11] and [6], the momentum equation $\mathbf{div}\,\boldsymbol{\sigma} = -\mathbf{f}$ is imposed in the L^2 sense at both the continuous and discrete levels. As discussed in [16], this enforcement comes at the expense of losing pressure robustness, which can be regarded as a trade-off for achieving momentum conservation.

The rest of the article is organized as follows: In Section 2, we introduce the three-field continuous problem and analyze its well-posedness. Then, in Section 3, we propose the numerical scheme and study its well-posedness and convergence. In Section 4 we address the extension to the Stokes problem with mixed boundary conditions. Finally, in 5 we illustrate the performance of the method by providing some numerical examples.

We conclude this section by introducing some notations and definitions. Throughout this work, we adopt standard notation for the Lebesgue and Sobolev spaces $\mathrm{L}^2(\Omega)$ and $\mathrm{H}^1(\Omega)$, equipped with the norms $\|\cdot\|_{0,\Omega}$ and $\|\cdot\|_{1,\Omega}$, respectively. The seminorm $|\cdot|_{1,\Omega}$ is also used for $\mathrm{H}^1(\Omega)$ and serves as a norm in the subspace $\mathrm{H}^1_0(\Omega)$ introduced earlier.

Furthermore, we use $\mathbf{S}$ and $\mathbb{S}$ to represent the vectorial and tensorial counterparts of a generic scalar function space S. For a vector field $\mathbf{v} = (v_i)_{i=1,d}$, the differential operators $\nabla\mathbf{v}$ and $\mathrm{div}\mathbf{v}$ employed above are defined as

$$\nabla\mathbf{v} := \left(\frac{\partial v_i}{\partial x_j}\right)_{i,j=1,d}, \quad \mathrm{div}\,\mathbf{v} := \sum_{j=1}^{d} \frac{\partial v_j}{\partial x_j}.$$

As usual, the spaces $\mathbf{H}(\mathrm{div};\Omega)$ and $\mathbb{H}(\mathbf{div}\,;\Omega)$ are equipped with the norms

$$\|\mathbf{v}\|_{\mathrm{div},\Omega} := \left(\|\mathbf{v}\|^2_{0,\Omega} + \|\mathrm{div}\,\mathbf{v}\|^2_{0,\Omega}\right)^{1/2}, \quad \|\boldsymbol{\tau}\|_{\mathbf{div}\,,\Omega} := \left(\|\boldsymbol{\tau}\|^2_{0,\Omega} + \|\mathbf{div}\,\boldsymbol{\tau}\|^2_{0,\Omega}\right)^{1/2},$$

respectively. Moreover, using [9, Lemma 2.3], it can be shown that the seminorm

$$|\boldsymbol{\tau}|_{\mathbf{div}\,,\Omega} := \left(\|\boldsymbol{\tau}^{\mathrm{d}}\|^2_{0,\Omega} + \|\mathbf{div}\,\boldsymbol{\tau}\|^2_{0,\Omega}\right)^{1/2}$$

is also a norm in $\mathbb{H}_0(\mathbf{div}\,;\Omega)$, equivalent to $\|\cdot\|_{\mathbf{div}\,,\Omega}$, that is, there exist $c_1, c_2 > 0$, such that

$$c_1\|\boldsymbol{\tau}\|_{\mathbf{div}\,,\Omega} \leq |\boldsymbol{\tau}|_{\mathbf{div}\,,\Omega} \leq c_2\|\boldsymbol{\tau}\|_{\mathbf{div}\,,\Omega}, \qquad \forall\,\boldsymbol{\tau} \in \mathbb{H}_0(\mathbf{div}\,;\Omega). \tag{1.8}$$

Finally, throughout our analysis, we will use C and c, with or without subscripts, bars, tildes, or hats, to denote generic positive constants independent of the discretization parameters. These constants may take different values in different contexts.

2 Continuous Problem

As previously mentioned, we introduce an equivalent reduced version of (1.6). To this end, we first redefine the pseudostress tensor as

$$\boldsymbol{\sigma} := \nabla\mathbf{u} - \frac{1}{\nu}p\,\mathbb{I} \quad \text{in } \Omega, \tag{2.1}$$

which leads to the ν-scaled version of (1.4):

$$\boldsymbol{\sigma}^{\mathrm{d}} = \nabla\mathbf{u} \quad \text{in } \Omega, \quad -\mathbf{div}\,\boldsymbol{\sigma} = \frac{1}{\nu}\mathbf{f} \quad \text{in } \Omega, \quad \mathbf{u} = \mathbf{u}_D \quad \text{on } \Gamma, \quad (\mathrm{tr}\,(\boldsymbol{\sigma}), 1)_\Omega = 0. \tag{2.2}$$

Notice that the pseudostress (2.1) is essentially a viscosity-scaled version of the tensor (1.3) introduced in [5] and [11]. We adopt this new definition of $\boldsymbol{\sigma}$ because, as we will see in Section 2, it ensures that the stability estimates for the associated bilinear forms remain valid with constants independent of the viscosity. Furthermore, this property guarantees that the theoretical

convergence rates for all unknowns are achieved with constants independent of ν. Based on this reasoning, for the remainder of this paper, we consider $\boldsymbol{\sigma}$ as defined in (2.1) and focus on deriving a finite element scheme that satisfies the conservation laws:

$$\operatorname{div} \mathbf{u} = 0 \quad \text{in } \Omega, \quad \text{and} \quad \mathbf{div}\, \boldsymbol{\sigma} = -\frac{1}{\nu}\mathbf{f} \quad \text{in } \Omega.$$

To achieve this, we introduce the following variational formulation based on (2.2): Find $\boldsymbol{\sigma} \in \mathbb{H}_0(\mathbf{div}\,;\Omega)$, $\mathbf{u} \in \mathbf{H}(\operatorname{div}^0;\Omega)$, and $\varphi \in \mathrm{H}^1_0(\Omega)$ such that

$$\begin{aligned} (\boldsymbol{\sigma}^{\mathrm{d}}, \boldsymbol{\tau}^{\mathrm{d}})_\Omega + (\mathbf{u} + \nabla\varphi, \mathbf{div}\, \boldsymbol{\tau})_\Omega &= \langle \boldsymbol{\tau}\mathbf{n}, \mathbf{u}_D\rangle_\Gamma\,, && \forall \boldsymbol{\tau} \in \mathbb{H}_0(\mathbf{div}\,;\Omega), \\ (\mathbf{v} + \nabla\psi, \mathbf{div}\, \boldsymbol{\sigma})_\Omega &= -\frac{1}{\nu}(\mathbf{f}, \mathbf{v} + \nabla\psi)_\Omega, && \forall\, (\mathbf{v}, \psi) \in \mathbf{H}(\operatorname{div}^0;\Omega) \times \mathrm{H}^1_0(\Omega). \end{aligned} \tag{2.3}$$

From the fact that $\mathbf{L}^2(\Omega) = \mathbf{H}(\operatorname{div}^0;\Omega) \oplus \mathrm{H}^1_0(\Omega)$, it is clear that, after scaling by ν, problems (1.6) and (2.3) are equivalent and consequently, problem (2.3) is well-posed. However, for the sake of completeness, in what follows we establish its unique solvability and stability.

As usual in the context of mixed problems, first we introduce the bilinear forms $\mathbf{a} : \mathbb{H}(\mathbf{div}\,;\Omega)\times \mathbb{H}(\mathbf{div}\,;\Omega) \to \mathbb{R}$, $\mathbf{b} : \mathbb{H}(\mathbf{div}\,;\Omega)\times(\mathbf{H}(\operatorname{div}^0;\Omega)\times\mathrm{H}^1_0(\Omega)) \to \mathbb{R}$ and the functionals $F : \mathbb{H}(\mathbf{div}\,;\Omega) \to \mathbb{R}$ and $G : \mathbf{H}(\operatorname{div}^0;\Omega) \times \mathrm{H}^1_0(\Omega) \to \mathbb{R}$, as follows:

$$\mathbf{a}(\boldsymbol{\sigma}, \boldsymbol{\tau}) := (\boldsymbol{\sigma}^{\mathrm{d}}, \boldsymbol{\tau}^{\mathrm{d}})_\Omega, \quad \mathbf{b}(\boldsymbol{\tau}, (\mathbf{v}, \psi)) := (\mathbf{div}\ \boldsymbol{\tau}, \mathbf{v} + \nabla\psi)_\Omega, \tag{2.4}$$

$$F(\boldsymbol{\tau}) := \langle \boldsymbol{\tau}\mathbf{n}, \mathbf{u}_D\rangle_\Gamma \quad \text{and} \quad G(\mathbf{v}, \psi) := -\frac{1}{\nu}(\mathbf{f}, \mathbf{v} + \nabla\psi)_\Omega. \tag{2.5}$$

Then, problem (2.3) can be rewritten with a mixed structure as follows: Find $(\boldsymbol{\sigma}, (\mathbf{u}, \varphi)) \in \mathbb{H}_0(\mathbf{div}\,;\Omega) \times (\mathbf{H}(\operatorname{div}^0;\Omega) \times \mathrm{H}^1_0(\Omega))$, such that:

$$\begin{aligned} \mathbf{a}(\boldsymbol{\sigma}, \boldsymbol{\tau}) + \mathbf{b}(\boldsymbol{\tau}, (\mathbf{u}, \varphi)) &= F(\boldsymbol{\tau}) && \forall\, \boldsymbol{\tau} \in \mathbb{H}_0(\mathbf{div}\,;\Omega), \\ \mathbf{b}(\boldsymbol{\sigma}, (\mathbf{v}, \psi)) &= G(\mathbf{v}, \psi) && \forall\, (\mathbf{v}, \psi) \in \mathbf{H}(\operatorname{div}^0;\Omega) \times \mathrm{H}^1_0(\Omega). \end{aligned} \tag{2.6}$$

The following theorem establishes the well-posedness of problem (2.6).

Theorem 2.1 *There exists a unique* $(\boldsymbol{\sigma}, (\mathbf{u}, \varphi)) \in \mathbb{H}_0(\mathbf{div}\,;\Omega) \times (\mathbf{H}(\operatorname{div}^0;\Omega) \times \mathrm{H}^1_0(\Omega))$ *solution to* (2.6) *with* $\varphi = 0$ *in* Ω. *Furthermore, there exists* $C > 0$, *independent of* ν, *such that*

$$|\boldsymbol{\sigma}|_{\mathbf{div},\Omega} + \|\mathbf{u}\|_{0,\Omega} \leq C\left(\frac{\|\mathbf{f}\|_{0,\Omega}}{\nu} + \|\mathbf{u}_D\|_{1/2,\Gamma}\right). \tag{2.7}$$

Proof. In what follows, we apply the classical Babuška–Brezzi theory (see [9, Theorem 2.3]) to establish the well-posedness of (2.6).

We begin by noting that, using the Cauchy–Schwarz inequality, estimate (1.8) and [9, Theorem 1.7], we can readily deduce that the bilinear forms $\mathbf{a}$ and $\mathbf{b}$, as well as the functionals G and F, satisfy the following boundedness estimates:

$$\begin{aligned} &|\mathbf{a}(\boldsymbol{\sigma}, \boldsymbol{\tau})| \leq |\boldsymbol{\sigma}|_{\mathbf{div},\Omega}|\boldsymbol{\tau}|_{\mathbf{div},\Omega}, && |\mathbf{b}(\boldsymbol{\tau}, (\mathbf{v}, \psi))| \leq |\boldsymbol{\tau}|_{\mathbf{div},\Omega}(\|\mathbf{v}\|_{\mathrm{div},\Omega} + |\psi|_{1,\Omega}), \\ &|G(\mathbf{v}, \psi)| \leq \frac{1}{\nu}\|\mathbf{f}\|_{0,\Omega}(\|\mathbf{v}\|_{\mathrm{div},\Omega} + |\psi|_{1,\Omega}), && |F(\boldsymbol{\tau})| \leq C\|\mathbf{u}_D\|_{1/2,\Gamma}|\boldsymbol{\tau}|_{\mathbf{div},\Omega}, \end{aligned} \tag{2.8}$$

where $C > 0$ is a constant independent of ν. Furthermore, a simple rescaling by ν allows us to deduce from [6, Lemma 2.3] that the following inf-sup condition holds:

$$\sup_{\mathbf{0}\neq\boldsymbol{\tau}\in\mathbb{H}_0(\mathbf{div};\Omega)} \frac{\mathbf{b}(\boldsymbol{\tau},(\mathbf{v},\psi))}{|\boldsymbol{\tau}|_{\mathbf{div},\Omega}} \geq \beta(\|\mathbf{v}\|_{\mathrm{div},\Omega} + |\psi|_{1,\Omega}) \qquad \forall\,(\mathbf{v},\psi)\in\mathbf{H}(\mathrm{div}^0;\Omega)\times \mathrm{H}^1_0(\Omega), \tag{2.9}$$

where $\beta > 0$ is a constant independent of ν.

Next, we define the kernel of $\mathbf{b}$ as

$$\mathbb{V} := \{\boldsymbol{\tau}\in\mathbb{H}_0(\mathbf{div};\Omega) : \mathbf{b}(\boldsymbol{\tau},(\mathbf{v},\psi)) = 0 \quad \forall\,(\mathbf{v},\psi)\in\mathbf{H}(\mathrm{div}^0;\Omega)\times\mathrm{H}^1_0(\Omega)\}.$$

Using the Helmholtz decomposition $\mathbf{L}^2(\Omega) = \mathbf{H}(\mathrm{div}^0;\Omega)\oplus \mathrm{H}^1_0(\Omega)$, it follows that $\mathbb{V}$ can be characterized as

$$\mathbb{V} = \{\boldsymbol{\tau}\in\mathbb{H}_0(\mathbf{div};\Omega) : \mathbf{div}\,\boldsymbol{\tau} = 0 \text{ in } \Omega\}.$$

Moreover, for each $\boldsymbol{\tau}\in\mathbb{V}$, the bilinear form $\mathbf{a}$ satisfies

$$\mathbf{a}(\boldsymbol{\tau},\boldsymbol{\tau}) = |\boldsymbol{\tau}|^2_{\mathbf{div},\Omega}, \tag{2.10}$$

which establishes the ellipticity of $\mathbf{a}$ on $\mathbb{V}$.

In this way, from (2.8), (2.9), (2.10) and the classical Babuška–Brezzi theory, we readily obtain the unique solvability of problem (2.6).

Now, to deduce that $\varphi = 0$ in Ω, given $\psi\in\mathrm{H}^1_0(\Omega)$, we simply take $\boldsymbol{\tau} = \big(\psi - |\Omega|^{-1}(\psi,1)_\Omega\big)\,\mathbb{I}\in\mathbb{H}_0(\mathbf{div};\Omega)$ in the first equation of (2.6) and recall that $\langle\mathbf{n},\mathbf{u}_D\rangle_\Gamma = 0$ (see (1.2)), to obtain

$$(\nabla\psi,\nabla\varphi)_\Omega = 0,$$

which together with the fact that ψ is arbitrary, implies that $\varphi = 0$ in Ω.

We conclude the proof by observing that estimate (2.7) is a direct consequence of the Babuška–Brezzi theory and the fact that $\varphi = 0$. □

3 Galerkin scheme

In this section, we introduce and analyze the mass and momentum conservative Galerkin scheme for the mixed formulation (2.6). Moreover, we derive the corresponding theoretical rates of convergence.

3.1 Discrete scheme

Let $\mathcal{T}_h$ be a regular family of regular triangulations of the polygonal region $\overline{\Omega}$ by triangles T in $\mathbb{R}^2$ or tetrahedra in $\mathbb{R}^3$ of diameter h_T, such that $\overline{\Omega} = \cup\{T : T\in\mathcal{T}_h\}$ and define $h := \max\{h_T : T\in\mathcal{T}_h\}$. Given an integer $l\geq 0$ and a subset S of $\mathbb{R}^d$, we denote by $P_l(S)$ the space of polynomials of total degree at most l defined on S. Hence, for each $T\in\mathcal{T}_h$, we define the local Raviart–Thomas space of lowest order and the Brezzi–Douglas–Marini (BDM) element of order 1, respectively as (see, for instance [4]):

$$\mathbf{RT}_0(T) := [P_0(T)]^d \oplus P_0(T)\mathbf{x} \quad \text{and} \quad \mathbf{BDM}_1(T) = [P_1(T)]^d$$

where $\mathbf{x} := (x_1,\ldots,x_d)^t$ is a generic vector of $\mathbb{R}^d$.

In addition, we let $\mathcal{E}_h$ be the set of edges (in 2D) or faces (in 3D) of $\mathcal{T}_h$, whose corresponding diameters are denoted h_e, and define

$$\mathcal{E}_h(\Omega) := \big\{ e \in \mathcal{E}_h : \quad e \subseteq \Omega \big\} \quad \text{and} \quad \mathcal{E}_h(\Gamma) := \big\{ e \in \mathcal{E}_h : \quad e \subseteq \Gamma \big\}.$$

We also let $[\![\cdot]\!]$ be the usual jump operator across internal edges or faces defined for piecewise continuous functions v, by

$$[\![v]\!] = (v|_{T_+})|_e - (v|_{T_-})|_e \quad \text{with} \quad e = \partial T_+ \cap \partial T_-,$$

where T_+ and T_- are the elements of $\mathcal{T}_h$ having e as a common edge or face. Then, we introduce the well-known Crouzeix–Raviart space (see [7]):

$$\begin{aligned} \Psi_h^{\varphi} := \quad \Big\{ & v_h : \Omega \to \mathbb{R} : v_h|_T \in P_1(T), \, \forall\, T \in \mathcal{T}_h, \quad \int_e [\![v_h]\!] = 0, \quad \forall\, e \in \mathcal{E}_h(\Omega) \\ & \text{and} \quad \int_e v_h = 0, \quad \forall e \in \mathcal{E}_h(\Gamma) \Big\}, \end{aligned} \tag{3.1}$$

equipped with the norm

$$|v_h|_h = \Big(\sum_{T \in \mathcal{T}_h} |v_h|_{1,T}^2 \Big)^{1/2}, \quad \forall v_h \in \Psi_h^{\varphi}.$$

In this way, defining the discrete spaces

$$\begin{aligned} \mathbb{H}_h^{\boldsymbol{\sigma}} &:= \{ \boldsymbol{\tau}_h \in \mathbb{H}(\mathbf{div}\,;\Omega) : \mathbf{c}^t \boldsymbol{\tau}_h \in \mathbf{BDM}_1(T) \quad \forall\, \mathbf{c} \in \mathbb{R}^d, \quad \forall\, T \in \mathcal{T}_h \}, \\ \mathbf{H}_h^{\mathbf{u}} &:= \{ \mathbf{z}_h \in \mathbf{H}(\mathrm{div};\Omega) : \mathbf{z}_h|_T \in \mathbf{RT}_0(T), \quad \forall\, T \in \mathcal{T}_h \}, \\ \mathbb{H}_{h,0}^{\boldsymbol{\sigma}} &:= \mathbb{H}_h^{\boldsymbol{\sigma}} \cap \mathbb{H}_0(\mathbf{div}\,;\Omega), \quad \mathbf{H}_{h,0}^{\mathbf{u}} := \mathbf{H}_h^{\mathbf{u}} \cap \mathbf{H}(\mathrm{div}^0;\Omega), \end{aligned} \tag{3.2}$$

the Galerkin scheme associated to (2.6) reads: Find $(\boldsymbol{\sigma}_h, (\mathbf{u}_h, \varphi_h)) \in \mathbb{H}_{h,0}^{\boldsymbol{\sigma}} \times (\mathbf{H}_{h,0}^{\mathbf{u}} \times \Psi_h^{\varphi})$, such that:

$$\begin{aligned} \mathbf{a}(\boldsymbol{\sigma}_h, \boldsymbol{\tau}_h) + \mathbf{b}_h(\boldsymbol{\tau}_h, (\mathbf{u}_h, \varphi_h)) &= F(\boldsymbol{\tau}_h) \qquad \forall\, \boldsymbol{\tau}_h \in \mathbb{H}_{h,0}^{\boldsymbol{\sigma}}, \\ \mathbf{b}_h(\boldsymbol{\sigma}_h, (\mathbf{v}_h, \psi_h)) &= G_h(\mathbf{v}_h, \psi_h) \quad \forall\, (\mathbf{v}_h, \psi_h) \in \mathbf{H}_{h,0}^{\mathbf{u}} \times \Psi_h^{\varphi}, \end{aligned} \tag{3.3}$$

where the form $\mathbf{a}$ and the functional F are defined in (2.4) and (2.5), respectively, whereas $\mathbf{b}_h : \mathbb{H}_0(\mathbf{div}\,;\Omega) \times \mathrm{H}(h) \to \mathbb{R}$ and the functional $G_h : \mathrm{H}(h) \to \mathbb{R}$ are defined as follows

$$\mathbf{b}_h(\boldsymbol{\tau}, (\mathbf{v}_h, \psi_h)) := (\mathbf{div}\ \boldsymbol{\tau}, \mathbf{v}_h + \nabla_h \psi_h)_\Omega, \tag{3.4}$$

$$G_h(\mathbf{v}_h, \psi_h) := -\frac{1}{\nu} (\mathbf{f}, \mathbf{v}_h + \nabla_h \psi_h)_\Omega, \tag{3.5}$$

where ∇_h is the discrete gradient for discontinuous functions, that is, $\nabla_h \psi_h|_T = \nabla(\psi_h|_T), \forall\, T \in \mathcal{T}_h$ and $\mathrm{H}(h) := \mathrm{H}_0^1(\Omega) + \Psi_h^{\varphi}$.

3.2 Well-posedness of the discrete scheme

In what follows we address the unique solvability and stability of problem (3.3) by adapting to the discrete case the analysis described in Section 2. We begin by noticing that using Hölder inequality, the form $\mathbf{b}_h$ and the functional G_h are bounded with the same constants as for $\mathbf{b}$ and G in (2.8).

Now we let $\mathbb{V}_h$ be discrete kernel of $\mathbf{b}_h$, that is

$$\mathbb{V}_h := \{\boldsymbol{\tau}_h \in \mathbb{X}_{h,0} : \ \mathbf{b}_h(\boldsymbol{\tau}_h, (\mathbf{v}_h, \psi_h)) = 0, \quad \forall\, (\mathbf{v}_h, \psi_h) \in \mathbf{H}^{\mathbf{u}}_{h,0} \times \Psi^{\varphi}_h\}.$$

Recalling from [2, Theorem 4.1] and [17, Theorem 4.9] that the following orthogonal decomposition holds:

$$\mathbf{Q}_h = \mathbf{H}^{\mathbf{u}}_{h,0} \oplus \nabla_h \Psi^{\varphi}_h, \tag{3.6}$$

where $\mathbf{Q}_h$ is the corresponding vectorial counterpart of the space

$$Q_h := \{q \in L^2(\Omega) \ : \ q|_T \in P_0(T), \quad \forall\, T \in \mathcal{T}_h\},$$

and

$$\nabla_h \Psi^{\varphi}_h := \{\mathbf{s}_h|_T \in \mathbf{P}_0(T) \ : \exists\, v_h \in \Psi^{\varphi}_h \text{ such that } \mathbf{s}_h|_T = \nabla(v_h|_T), \quad \forall\, T \in \mathcal{T}_h\},$$

we observe that for each $\boldsymbol{\tau}_h \in \mathbb{V}_h$,

$$(\mathbf{div}\ \boldsymbol{\tau}_h, \mathbf{v}_h + \nabla_h \psi_h)_\Omega = 0, \quad \forall\, (\mathbf{v}_h, \psi_h) \in \mathbf{H}^{\mathbf{u}}_{h,0} \times \Psi^{\varphi}_h,$$

is equivalent to

$$(\mathbf{div}\ \boldsymbol{\tau}_h, \mathbf{z}_h)_\Omega = 0, \quad \forall\, \mathbf{z}_h \in \mathbf{Q}_h,$$

which implies that $\mathbb{V}_h$ can be characterized as follows

$$\mathbb{V}_h := \{\boldsymbol{\tau}_h \in \mathbb{X}_{h,0} : \mathbf{div}\, \boldsymbol{\tau}_h = \mathbf{0} \quad \text{in} \quad \Omega\}.$$

In this way, $\mathbf{a}$ satisfies

$$\mathbf{a}(\boldsymbol{\tau}_h, \boldsymbol{\tau}_h) = |\boldsymbol{\tau}_h|^2_{\mathbf{div},\Omega} \qquad \forall \boldsymbol{\tau}_h \in \mathbb{V}_h,$$

that is, $\mathbf{a}$ is elliptic on the kernel of $\mathbf{b}_h$.

Now we establish the discrete inf-sup condition of $\mathbf{b}_h$. To that end, we recall from [4, Section 2.5] that there exist interpolator operators $\Pi^{RT}_h : \mathbf{H}^1(\Omega) \to \mathbf{H}^{\mathbf{u}}_h$ and $\Pi^{BDM}_h : \mathbf{H}^1(\Omega) \to \mathbf{X}_h := \{\tau_h \in \mathbf{H}(\mathrm{div};\Omega) : \tau_h|_T \in \mathbf{BDM}_1(T), \quad \forall\, T \in \mathcal{T}_h\}$, satisfying the approximation property

$$\|\Pi^{\star}_h(\tau) - \tau\|_{0,T} \leq c h^m_T |\tau|_{m,T}, \quad \forall \tau \in \mathbf{H}^m(T), \quad \forall\, T \in \mathcal{T}_h, \tag{3.7}$$

for all $1 \leq m \leq l_\star$ and $\star \in \{RT, BDM\}$, with $l_{RT} = 1$ and $l_{BDM} = 2$, and the commutative property

$$\mathrm{div}(\Pi^{\star}_h(\tau)) = \mathcal{P}_h(\mathrm{div}\,\tau), \quad \forall \tau \in \mathbf{H}^1(\Omega), \quad \forall \star \in \{RT, BDM\}, \tag{3.8}$$

where $\mathcal{P}_h$ is the L^2-projection on Q_h, which satisfies

$$(\mathcal{P}_h(v) - v, z_h)_\Omega = 0 \quad \forall\, z_h \in Q_h,$$

and the local approximation property

$$\|v - \mathcal{P}_h(v)\|_{0,T} \leq C h^m |v|_{m,T}, \quad \forall\, T \in \mathcal{T}_h, \tag{3.9}$$

for all $0 \leq m \leq 1$ and for all $v \in \mathrm{H}^m(\Omega)$. Notice that from (3.8) and (3.9) we have that

$$\|\mathrm{div}\,\tau - \mathrm{div}(\Pi_h^\star(\tau))\|_{0,T} \leq Ch^m |\mathrm{div}\,\tau|_{m,T}, \quad \forall\, T \in \mathcal{T}_h,$$

for all $0 \leq m \leq 1$ and for all $\tau \in \mathbf{H}^1(\Omega)$ with $\mathrm{div}\,\tau \in \mathrm{H}^m(\Omega)$.

In what follows we will employ a tensor version of Π_h^{BDM}, denoted by $\boldsymbol{\Pi}_h^{BDM} : \mathbb{H}^1(\Omega) \to \mathbb{H}_h^{\boldsymbol{\sigma}}$, which is defined row-wise by Π_h^{BDM}, and the vector version of $\mathcal{P}_h$, denoted by $\mathbf{P}_h : \mathbf{L}^2(\Omega) \to \mathbf{Q}_h$, defined component-wise by $\mathcal{P}_h$.

Now we are in position of establishing the inf-sup condition of $\mathbf{b}_h$.

Lemma 3.1 *There exists $\tilde{\beta} > 0$, independent of h and ν, such that*

$$\sup_{\mathbf{0} \neq \boldsymbol{\tau}_h \in \mathbb{H}_{h,0}^{\boldsymbol{\sigma}}} \frac{\mathbf{b}_h(\boldsymbol{\tau}_h, (\mathbf{v}_h, \psi_h))}{|\boldsymbol{\tau}_h|_{\mathbf{div},\Omega}} \geq \tilde{\beta}(\|\mathbf{v}_h\|_{\mathrm{div},\Omega} + |\psi_h|_h) \qquad \forall\, (\mathbf{v}_h, \psi_h) \in \mathbf{H}_{h,0}^{\mathbf{u}} \times \Psi_h^{\varphi}.$$

Proof. We proceed similary to the proof of [6, Lemma 3.2]. In fact, we let $B \subseteq \mathbb{R}^d$ be a bounded and open convex domain such that $\overline{\Omega} \subset B$, and given $(\mathbf{v}_h, \psi_h) \in \mathbf{H}_{h,0}^{\mathbf{u}} \times \Psi_h^{\varphi}$, we let $\mathbf{z} \in \mathbf{H}_0^1(B)$ be the unique weak solution of the auxiliary problem

$$-\Delta \mathbf{z} = \mathbf{h}(\mathbf{v}_h, \psi_h) \quad \text{in} \quad B, \quad \mathbf{z} = \mathbf{0} \quad \text{on} \quad \partial B,$$

with

$$\mathbf{h}(\mathbf{v}_h, \psi_h) := \begin{cases} \mathbf{v}_h + \nabla_h \psi_h, & \text{in} \quad \Omega, \\ \mathbf{0}, & \text{in} \quad B \backslash \overline{\Omega}. \end{cases}$$

It is well known that $\mathbf{z} \in \mathbf{H}^2(B)$ (see [12]) and

$$\|\mathbf{z}\|_{2,\Omega} \leq C\|\mathbf{h}(\mathbf{v}_h, \psi_h)\|_{0,B} = C\|\mathbf{v}_h + \nabla_h \psi_h\|_{0,\Omega} \leq C\left(\|\mathbf{v}_h\|_{\mathrm{div},\Omega} + |\psi_h|_h\right). \tag{3.10}$$

Note that as $\mathbf{v}_h \in \mathbf{H}_{h,0}^{\mathbf{u}}$, then in accordance with [4, Corollary 2.3.1], $\mathbf{v}_h \in \mathbf{Q}_h$. Now, we define

$$\widehat{\boldsymbol{\tau}}_h := -\boldsymbol{\Pi}_h^{BDM}(\nabla \mathbf{z}|_\Omega) + \frac{1}{d|\Omega|}\left(\mathrm{tr}\,(\boldsymbol{\Pi}_h^{BDM}(\nabla \mathbf{z}|_\Omega)), 1\right)_\Omega \mathbb{I} \quad \text{in} \quad \Omega,$$

and observe from (3.8) and (3.10) that

$$\mathbf{div}\,\widehat{\boldsymbol{\tau}}_h = \mathbf{v}_h + \nabla_h \psi_h \in \mathbf{Q}_h \quad \text{and} \quad |\widehat{\boldsymbol{\tau}}_h|_{\mathbf{div},\Omega} \leq \hat{C}(\|\mathbf{v}_h\|_{\mathrm{div},\Omega} + |\psi_h|_h).$$

From the latter, we obtain

$$\sup_{\mathbf{0} \neq \boldsymbol{\tau}_h \in \mathbb{H}_{h,0}^{\boldsymbol{\sigma}}} \frac{\mathbf{b}_h(\boldsymbol{\tau}_h, (\mathbf{v}_h, \psi_h))}{|\boldsymbol{\tau}_h|_{\mathbf{div},\Omega}} \geq \frac{\mathbf{b}(\widehat{\boldsymbol{\tau}}_h, (\mathbf{v}_h, \psi_h))}{|\widehat{\boldsymbol{\tau}}_h|_{\mathbf{div},\Omega}} \geq \hat{C}^{-1} \frac{\|\mathbf{v}_h\|_{\mathrm{div},\Omega}^2 + |\psi_h|_h^2}{\|\mathbf{v}_h\|_{\mathrm{div},\Omega} + |\psi_h|_h} \geq \tilde{\beta}(\|\mathbf{v}_h\|_{\mathrm{div},\Omega} + |\psi_h|_h), \tag{3.11}$$

with $\tilde{\beta} > 0$ independent of h and ν.

□

These properties and the Babuška–Brezzi theory allow us to conclude the well-posedness of (3.3). This result is summarized in the following theorem.

Theorem 3.2 *There exists a unique $(\boldsymbol{\sigma}_h, (\mathbf{u}_h, \varphi_h)) \in \mathbb{H}_{h,0}^{\boldsymbol{\sigma}} \times (\mathbf{H}_{h,0}^{\mathbf{u}} \times \Psi_h^{\varphi})$ solution to the Galerkin scheme* (3.3)*. In addition, there exists $C > 0$, independent of h and ν, such that*

$$|\boldsymbol{\sigma}_h|_{\mathbf{div},\Omega} + \|\mathbf{u}_h\|_{0,\Omega} + |\varphi_h|_h \leq C\left(\frac{\|\mathbf{f}\|_{0,\Omega}}{\nu} + \|\mathbf{u}_D\|_{1/2,\Omega}\right).$$

Remark 3.3 *Observe that the discrete space* $\mathbf{H}^{\mathbf{u}}_{h,0}$ *becomes*

$$\mathbf{H}^{\mathbf{u}}_{h,0} = \{\mathbf{v}_h \in \mathbf{H}^{\mathbf{u}}_h : \operatorname{div} \mathbf{v}_h = 0 \text{ in } \Omega\},$$

which implies that the numerical scheme (3.3) *produces exactly divergence-free approximations for the velocity* $\mathbf{u}$.

Furthermore, from the second equation of (3.3) *and the discrete Helmholtz decomposition* (3.6)*, we deduce that*

$$\big(\mathbf{div}\ \boldsymbol{\sigma}_h + \nu^{-1}\mathbf{f}, \mathbf{z}_h\big)_\Omega = 0 \quad \forall\, \mathbf{z}_h \in \mathbf{Q}_h.$$

This implies that $\mathbf{div}\ \boldsymbol{\sigma}_h = -\nu^{-1}\mathbf{P}_h(\mathbf{f})$*, meaning that the method exactly preserves the discrete equilibrium equation when* $\mathbf{f} \in \mathbf{Q}_h$*. In other words, the scheme is momentum conservative whenever* $\mathbf{f} \in \mathbf{Q}_h$*. Moreover, if* $\mathbf{f} \in \mathbf{H}^1(\Omega)$*, from* (3.9) *we obtain the estimate*

$$\|\nu^{-1}\mathbf{f} + \mathbf{div}\ \boldsymbol{\sigma}_h\|_{0,\Omega} = \nu^{-1}\|\mathbf{f} - \mathbf{P}_h(\mathbf{f})\|_{0,\Omega} \leq c\nu^{-1}h\|\mathbf{f}\|_{1,\Omega}, \tag{3.12}$$

showing that, for sufficiently smooth $\mathbf{f}$*, the momentum equation is approximated with an optimal rate of convergence.*

We also emphasize that the achieved momentum conservation comes at the cost of losing pressure robustness. More specifically, since our method enforces the equilibrium equation in $\mathbf{L}^2(\Omega)$*, the gradient component of the Helmholtz decomposition of the source term* $\mathbf{f}$ *affects the solution, leading to a lack of pressure robustness, as discussed in [16].*

On the other hand, note that if $(\boldsymbol{\sigma}_h, (\mathbf{u}_h, \varphi_h))$ *is a solution to* (3.3)*,* φ_h *is not necessarily identically zero in* Ω*. However, as shown in Theorem 3.4,* φ_h *converges to zero (see* (3.16)*). Furthermore, as demonstrated in Example 4, Section 5, despite introducing an additional unknown, the proposed numerical scheme remains slightly less expensive than the standard formulation studied in [5] and [11]. The computational cost can be further reduced by employing the exactly divergence-free discrete basis for* $\mathbf{H}^{\mathbf{u}}_{h,0}$ *introduced in [1], optimizing implementation efficiency.*

Finally, we note that, to the best of the authors' knowledge, the Helmholtz decomposition (3.6) *is only available in the literature for the lowest-order case. This limitation prevents a straightforward extension of the above analysis to higher-order cases.*

3.3 Convergence analysis

We now analyze the convergence of (3.1) and establish the corresponding theoretical rate of convergence. We begin by noting that the gradient operator ∇ and its discrete counterpart ∇_h coincide in $\mathrm{H}^1_0(\Omega)$, which implies that

$$\mathbf{b}_h(\boldsymbol{\tau}, (\mathbf{v}, \psi)) = \mathbf{b}(\boldsymbol{\tau}, (\mathbf{v}, \psi)), \qquad \forall\, (\boldsymbol{\tau}, (\mathbf{v}, \psi)) \in \mathbb{H}(\mathbf{div}\,; \Omega) \times (\mathbf{H}(\mathrm{div}^0; \Omega) \times \mathrm{H}^1_0(\Omega)), \tag{3.13}$$

and

$$G_h(\mathbf{v}, \psi) = G(\mathbf{v}, \psi), \qquad \forall\, (\mathbf{v}, \psi) \in \mathbf{H}(\mathrm{div}^0; \Omega) \times \mathrm{H}^1_0(\Omega). \tag{3.14}$$

Thus, if $(\boldsymbol{\sigma}, (\mathbf{u}, \varphi)) \in \mathbb{H}(\mathbf{div}\,; \Omega) \times (\mathbf{H}(\mathrm{div}^0; \Omega) \times \mathrm{H}^1_0(\Omega))$ is the unique solution of (2.6), we can replace $\mathbf{b}$ with $\mathbf{b}_h$ and G with G_h in (2.6) without altering the validity of the equations.

The following theorem establishes the theoretical rate of convergence for the numerical scheme (3.3). Instead of relying on the *a priori* error estimate given, for instance, in [9, Theorem 2.6], we derive the estimate from scratch, utilizing the orthogonality property of the scheme.

This approach allows us to obtain error bounds with constants independent of ν, which, as we shall see, differs from the results in [6]. Moreover, it allows us to establish a superconvergence result for the deviatoric part of $\boldsymbol{\sigma}_h$.

Theorem 3.4 *Let $(\boldsymbol{\sigma},(\mathbf{u},0)) \in \mathbb{H}_0(\mathbf{div}\,;\Omega)\times(\mathbf{H}(\mathrm{div}^0;\Omega)\times \mathrm{H}^1_0(\Omega))$ and $(\boldsymbol{\sigma}_h,(\mathbf{u}_h,\varphi_h)) \in \mathbb{H}^{\boldsymbol{\sigma}}_{h,0}\times \mathbf{H}^{\mathbf{u}}_{h,0}\times\Psi^{\varphi}_h$ be the unique solutions of (2.6) and (3.3), respectively, and assume that the exact solution satisfies $\boldsymbol{\sigma}\in\mathbb{H}^2(\Omega)$ and $\mathbf{u}\in\mathbf{H}^1(\Omega)$, Then, there exist positive constants c_1, c_2 and c_3, independent of ν and h, such that,*

$$\|\boldsymbol{\sigma}^{\mathrm{d}}-\boldsymbol{\sigma}^{\mathrm{d}}_h\|_{0,\Omega} \,\leq\, c_1 h^2|\boldsymbol{\sigma}|_{2,\Omega} \tag{3.15}$$

and

$$\|\mathbf{u}-\mathbf{u}_h\|_{0,\Omega}+|\varphi_h|_h \,\leq\, c_2 h|\boldsymbol{\sigma}|_{2,\Omega} \,+\, c_3 h|\mathbf{u}|_{1,\Omega}. \tag{3.16}$$

Proof. From (2.6), (3.3), (3.13), (3.14) and the fact that $\varphi = 0$ in Ω, we readily obtain the orthogonality property:

$$\begin{aligned}((\boldsymbol{\sigma}-\boldsymbol{\sigma}_h)^{\mathrm{d}},\boldsymbol{\tau}^{\mathrm{d}}_h)_\Omega+(\mathbf{u}-\mathbf{u}_h-\nabla_h\varphi_h,\mathbf{div}\,\boldsymbol{\tau}_h)_\Omega &= \;\; 0, \quad \forall\boldsymbol{\tau}_h\in\mathbb{H}^{\boldsymbol{\sigma}}_{h,0},\\ (\mathbf{v}_h+\nabla_h\psi_h,\mathbf{div}\,(\boldsymbol{\sigma}-\boldsymbol{\sigma}_h))_\Omega &= \;\; 0, \quad \forall(\mathbf{v}_h,\psi_h)\in\mathbf{H}^{\mathbf{u}}_{h,0}\times\Psi^{\varphi}_h.\end{aligned} \tag{3.17}$$

Now, let $\widehat{\boldsymbol{\sigma}}_h := \boldsymbol{\Pi}^{BDM}_h(\boldsymbol{\sigma})$ and $\widehat{\mathbf{u}}_h := \Pi^{RT}_h(\mathbf{u})$. From (3.8) and using that $\mathbf{div}\,\boldsymbol{\sigma} = -\frac{1}{\nu}\mathbf{f}$ in Ω and $\mathbf{div}\,\boldsymbol{\sigma}_h = -\frac{1}{\nu}\mathbf{P}_h(\mathbf{f})$ in Ω (see Remark 3.3), it is clear that

$$\mathbf{div}\,(\widehat{\boldsymbol{\sigma}}_h)=\mathbf{P}_h(\mathbf{div}\,\boldsymbol{\sigma})=-\frac{1}{\nu}\mathbf{P}_h(\mathbf{f})=\mathbf{div}\,(\boldsymbol{\sigma}_h)\quad\text{in}\quad\Omega,$$

thus $\mathbf{div}\,(\widehat{\boldsymbol{\sigma}}_h-\boldsymbol{\sigma}_h)=\mathbf{0}$ in Ω. Then, adding and subtracting $\widehat{\boldsymbol{\sigma}}_h$ in the first equation of (3.17) and taking $\boldsymbol{\tau}_h=\widehat{\boldsymbol{\sigma}}_h-\boldsymbol{\sigma}_h$, we deduce that

$$((\widehat{\boldsymbol{\sigma}}_h-\boldsymbol{\sigma}_h)^{\mathrm{d}},(\widehat{\boldsymbol{\sigma}}_h-\boldsymbol{\sigma}_h)^{\mathrm{d}})_\Omega=-((\boldsymbol{\sigma}-\widehat{\boldsymbol{\sigma}}_h)^{\mathrm{d}},(\widehat{\boldsymbol{\sigma}}_h-\boldsymbol{\sigma}_h)^{\mathrm{d}})_\Omega,$$

which implies

$$\|(\widehat{\boldsymbol{\sigma}}_h-\boldsymbol{\sigma}_h)^{\mathrm{d}}\|_{0,\Omega}\leq\|(\boldsymbol{\sigma}-\widehat{\boldsymbol{\sigma}}_h)^{\mathrm{d}}\|_{0,\Omega}.$$

In this way, from the latter, the triangle inequality, estimate (3.7) and the regularity of the mesh, we deduce that

$$\|(\boldsymbol{\sigma}-\boldsymbol{\sigma}_h)^{\mathrm{d}}\|_{0,\Omega}\leq 2\|(\boldsymbol{\sigma}-\widehat{\boldsymbol{\sigma}}_h)^{\mathrm{d}}\|_{0,\Omega}\leq 2\|\boldsymbol{\sigma}-\widehat{\boldsymbol{\sigma}}_h\|_{0,\Omega}\leq c_1h^2\|\boldsymbol{\sigma}\|_{2,\Omega},$$

with $c_1>0$ in dependent of h and ν.

Now, to deduce (3.16) we add and subtract $\widehat{\mathbf{u}}_h$ in the first equation of (3.17) to obtain

$$(\widehat{\mathbf{u}}_h-\mathbf{u}_h-\nabla_h\varphi_h,\mathbf{div}\,\boldsymbol{\tau}_h)_\Omega=-(\mathbf{u}-\widehat{\mathbf{u}}_h,\mathbf{div}\,\boldsymbol{\tau}_h)_\Omega-((\boldsymbol{\sigma}-\boldsymbol{\sigma}_h)^{\mathrm{d}},\boldsymbol{\tau}^{\mathrm{d}}_h)_\Omega,$$

for all $\boldsymbol{\tau}_h\in\mathbb{H}^{\boldsymbol{\sigma}}_{h,0}$. Then, from this identity and the discrete inf-sup condition (3.11) we obtain

$$\begin{aligned}\widetilde{\beta}(\|\widehat{\mathbf{u}}_h-\mathbf{u}_h\|_{0,\Omega}+|\varphi_h|_h) &\leq \sup_{\mathbf{0}\neq\boldsymbol{\tau}_h\in\mathbb{H}^{\boldsymbol{\sigma}}_{h,0}}\frac{\big|(\mathbf{u}-\widehat{\mathbf{u}}_h,\mathbf{div}\,\boldsymbol{\tau}_h)_\Omega+((\boldsymbol{\sigma}-\boldsymbol{\sigma}_h)^{\mathrm{d}},\boldsymbol{\tau}^{\mathrm{d}}_h)_\Omega\big|}{|\boldsymbol{\tau}_h|_{\mathbf{div}\,,\Omega}},\\ &\leq C(\|\mathbf{u}-\widehat{\mathbf{u}}_h\|_{0,\Omega}+\|(\boldsymbol{\sigma}-\boldsymbol{\sigma}_h)^{\mathrm{d}}\|_{0,\Omega}),\end{aligned}$$

which combined with (3.7), (3.15) and the triangle inequality imply (3.16). □

Remark 3.5 *Recalling that* $\boldsymbol{\sigma}^{\mathrm{d}} = \nabla \mathbf{u}$*, the previous theorem confirms that the method provides a superconvergent approximation for the velocity gradient. Specifically, we obtain the following estimate:*

$$\|\nabla \mathbf{u} - \boldsymbol{\sigma}_h^{\mathrm{d}}\|_{0,\Omega} \leq c_1 h^2 |\boldsymbol{\sigma}|_{2,\Omega},$$

where c_1 *is independent of* ν*.*

4 Stokes problem with mixed boundary conditions

Now we briefly discuss how to extend the method for the case of mixed boundary conditions. To that end, now we let $\Gamma_D \subseteq \partial\Omega$ and $\Gamma_N \subseteq \partial\Omega$ satisfying $|\Gamma_N| \neq 0$, $|\Gamma_D| \neq 0$, $\Gamma_D \cap \Gamma_N = \emptyset$ and $\overline{\Gamma}_D \cup \overline{\Gamma}_N = \partial\Omega$, and consider the following Stokes problem with mixed boundary conditions:

$$-\nu\Delta\mathbf{u} + \nabla p = \mathbf{f} \quad \text{in } \Omega, \quad \operatorname{div}\mathbf{u} = 0 \quad \text{in } \Omega, \quad \mathbf{u} = \mathbf{u}_D \quad \text{on } \Gamma_D, \quad (\nu\nabla\mathbf{u} - p\mathbb{I})\mathbf{n} = \mathbf{0} \quad \text{on } \Gamma_N,$$

where the last equation on Γ_N is the so-called *do-nothing* condition (see eg. [14, Section 2.4]).

Introducing the pseudostress tensor (2.1) the equations above can be rewritten equivalently as follows:

$$\boldsymbol{\sigma}^{\mathrm{d}} = \nabla\mathbf{u} \quad \text{in } \Omega, \quad -\mathbf{div}\,\boldsymbol{\sigma} = \frac{1}{\nu}\mathbf{f} \quad \text{in } \Omega, \quad \mathbf{u} = \mathbf{u}_D \quad \text{on} \quad \Gamma_D, \quad \boldsymbol{\sigma}\mathbf{n} = \mathbf{0} \quad \text{on} \quad \Gamma_N, \tag{4.1}$$

which lead to the variational formulation: Find $\boldsymbol{\sigma} \in \mathbb{H}_N(\mathbf{div}\,;\Omega)$, $\mathbf{u} \in \mathbf{H}(\mathrm{div}^0;\Omega)$ and $\varphi \in \mathrm{H}_0^1(\Omega)$, such that

$$\begin{aligned} \mathbf{a}(\boldsymbol{\sigma},\boldsymbol{\tau}) + \mathbf{b}(\boldsymbol{\tau},(\mathbf{u},\varphi)) &= F_D(\boldsymbol{\tau}), \quad \forall \boldsymbol{\tau} \in \mathbb{H}_N(\mathbf{div}\,;\Omega), \\ \mathbf{b}(\boldsymbol{\sigma},(\mathbf{v},\psi)) &= G(\mathbf{v},\psi), \quad \forall (\mathbf{v},\psi) \in \mathbf{H}(\mathrm{div}^0;\Omega) \times \mathrm{H}_0^1(\Omega), \end{aligned} \tag{4.2}$$

where $\mathbf{a}$, $\mathbf{b}$ and G are defined in (2.4) and (2.5), whereas $F_D : \mathbb{H}_N(\mathbf{div}\,;\Omega) \to \mathbb{R}$ si given by

$$F_D(\boldsymbol{\tau}) := \langle \boldsymbol{\tau}\mathbf{n}, \mathbf{u}_D \rangle_{\Gamma_D}, \tag{4.3}$$

with

$$\mathbb{H}_N(\mathbf{div}\,;\Omega) := \{\boldsymbol{\tau} \in \mathbb{H}(\mathbf{div}\,;\Omega) \,:\, \boldsymbol{\tau}\mathbf{n} = \mathbf{0} \quad \text{on} \quad \Gamma_N\},$$

and $\langle\cdot,\cdot\rangle_{\Gamma_D}$ denoting the product of duality between the trace space $\mathbf{H}^{1/2}(\Gamma_D)$ and its dual $\mathbf{H}^{-1/2}(\Gamma_D)$.

The well-posedness of (4.2) is established next.

Theorem 4.1 *There exists a unique* $(\boldsymbol{\sigma},(\mathbf{u},\varphi)) \in \mathbb{H}_N(\mathbf{div}\,;\Omega) \times (\mathbf{H}(\mathrm{div}^0;\Omega) \times \mathrm{H}_0^1(\Omega))$ *solution to* (4.2) *with* $\varphi = 0$ *in* Ω*. Furthermore, there exists* $C > 0$*, independent of* ν*, such that*

$$|\boldsymbol{\sigma}|_{\mathbf{div},\Omega} + \|\mathbf{u}\|_{\mathrm{div},\Omega} \leq C\left(\frac{\|\mathbf{f}\|_{0,\Omega}}{\nu} + \|\mathbf{u}_D\|_{1/2,\Gamma_D}\right). \tag{4.4}$$

Proof. Employing similar arguments to those utilized in the proof of Theorem 2.1 it is possible to prove existence and uniqueness of solution of problem (4.2) and estimate (4.4). In particular, the ellipticity of the bilinear form $\mathbf{a}$ on the kernel of $\mathbf{b}$ can be derived by combining (1.8) and [9, Lemma 2.5]. In addition, by taking $\boldsymbol{\tau} = \psi\mathbb{I} \in \mathbb{H}_N(\mathbf{div}\,;\Omega)$ with $\psi \in \mathrm{H}_0^1(\Omega)$ in the second

equation of (4.2), and proceeding analogously to the proof of Theorem 2.1 we easily prove that $\varphi = 0$ in Ω. We omit further details. $\square$

As for the Galerkin discretization of problem (4.2), here we consider the spaces defined in (3.1) and (3.2) and additionally let

$$\mathbb{H}^{\boldsymbol{\sigma}}_{h,N} := \mathbb{H}^{\boldsymbol{\sigma}}_h \cap \mathbb{H}_N(\mathbf{div}\,;\Omega).$$

Then, the mass and momentum conservative Galerkin scheme associated to (4.2) reads: Find $(\boldsymbol{\sigma}_h, (\mathbf{u}_h, \varphi_h)) \in \mathbb{H}^{\boldsymbol{\sigma}}_{h,N} \times (\mathbf{H}^{\mathbf{u}}_{h,0} \times \Psi^{\varphi}_h)$, such that

$$\begin{aligned} \mathbf{a}(\boldsymbol{\sigma}_h, \boldsymbol{\tau}_h) + \mathbf{b}_h(\boldsymbol{\tau}_h, (\mathbf{u}_h, \varphi_h)) &= F_D(\boldsymbol{\tau}_h) \qquad \forall\, \boldsymbol{\tau}_h \in \mathbb{H}^{\boldsymbol{\sigma}}_{h,N}, \\ \mathbf{b}_h(\boldsymbol{\sigma}_h, (\mathbf{v}_h, \psi_h)) &= G_h(\mathbf{v}_h, \psi_h) \quad \forall\, (\mathbf{v}_h, \psi_h) \in \mathbf{H}^{\mathbf{u}}_{h,0} \times \Psi^{\varphi}_h, \end{aligned} \tag{4.5}$$

where the form $\mathbf{a}$ is defined in (2.4), $\mathbf{b}_h$ and G_h are defined in (3.4) and (3.5), respectively, and the functional F_D is given by (4.3).

The well-posedness of (4.5), along with the derivation of the optimal convergence rates, can be established with minor modifications to the analysis presented in Sections 3.2 and 3.3. The following theorem summarizes these results, with the proofs omitted for brevity.

Theorem 4.2 *There exists a unique* $(\boldsymbol{\sigma}_h, (\mathbf{u}_h, \varphi_h)) \in \mathbb{H}^{\boldsymbol{\sigma}}_{h,N} \times (\mathbf{H}^{\mathbf{u}}_{h,0} \times \Psi^{\varphi}_h)$ *solution to the Galerkin scheme* (3.3)*. In addition, there exists* $C > 0$*, independent of* h *and* ν*, such that*

$$|\boldsymbol{\sigma}_h|_{\mathbf{div}\,,\Omega} + \|\mathbf{u}_h\|_{0,\Omega} + |\varphi_h|_h \leq C\Big(\frac{\|\mathbf{f}\|_{0,\Omega}}{\nu} + \|\mathbf{u}_D\|_{1/2,\Gamma_D} \Big).$$

In addition, if $(\boldsymbol{\sigma}, (\mathbf{u}, 0)) \in \mathbb{H}_N(\mathbf{div}\,;\Omega) \times (\mathbf{H}(\mathrm{div}^0;\Omega) \times \mathrm{H}^1_0(\Omega))$ *is the unique solution of* (4.2) *satisfying* $\boldsymbol{\sigma} \in \mathbb{H}^2(\Omega)$ *and* $\mathbf{u} \in \mathbf{H}^1(\Omega)$*, then there exist positive constants* $\tilde{c}_1$*,* $\tilde{c}_2$ *and* $\tilde{c}_3$ *independent of* ν *and* h*, such that,*

$$\|\boldsymbol{\sigma}^{\mathrm{d}} - \boldsymbol{\sigma}^{\mathrm{d}}_h\|_{0,\Omega} \leq \tilde{c}_1 h^2 |\boldsymbol{\sigma}|_{2,\Omega}$$

and

$$\|\mathbf{u} - \mathbf{u}_h\|_{0,\Omega} + |\varphi_h|_h \leq \tilde{c}_2 h |\boldsymbol{\sigma}|_{2,\Omega} + \tilde{c}_3 h |\mathbf{u}|_{1,\Omega}.$$

5 Numerical tests

In this section we present four numerical examples illustrating the performance of our finite element scheme and confirming the theoretical rates of convergence. We begin by mentioning that the numerical results that follow are attained by imposing the condition of $(\mathrm{tr}\,(\boldsymbol{\sigma}_h), 1)_\Omega = 0$ through a penalty strategy using a scalar Lagrange multiplier (adding one row and one column to the system). Also, the divergence-free constraint for the velocity is imposed by means of an appropriate Lagrange multiplier $r_h \in Q_h$. More precisely, we replace the numerical scheme (3.3) by the system: Find $(\boldsymbol{\sigma}_h, \mathbf{u}_h, \varphi_h, r_h, \lambda_h) \in \mathbb{H}^{\boldsymbol{\sigma}}_{h,0} \times \mathbf{H}^{\mathbf{u}}_{h,0} \times \Psi_h \times Q_h \times \mathbb{R}$, such that:

$$\begin{aligned} \mathbf{a}(\boldsymbol{\sigma}_h, \boldsymbol{\tau}_h) + \mathbf{b}_h(\boldsymbol{\tau}_h, (\mathbf{u}_h, \varphi_h)) + \lambda_h(\mathrm{tr}\,(\boldsymbol{\tau}_h), 1)_\Omega &= F(\boldsymbol{\tau}_h), \\ \mathbf{b}_h(\boldsymbol{\sigma}_h, (\mathbf{v}_h, \psi_h)) + (r_h, \mathrm{div}\,\mathbf{v}_h)_\Omega &= G(\mathbf{v}_h, \psi_h), \\ (s_h, \mathrm{div}\,\mathbf{u}_h)_\Omega &= 0, \\ \eta_h(\,\mathrm{tr}\,(\boldsymbol{\sigma}_h), 1)_\Omega &= 0, \end{aligned}$$

for all $(\boldsymbol{\tau}_h, \mathbf{v}_h, \psi_h, s_h, \eta_h) \in \mathbb{H}^{\boldsymbol{\sigma}}_{h,0} \times \mathbf{H}^{\mathbf{u}}_{h,0} \times \Psi^{\varphi}_h \times Q_h \times \mathbb{R}$. Our implementation is based on *Freefem++* code (see [13]), in conjunction with the direct linear solver UMFPACK (see [8]).

Now we introduce some additional notations. In what follows, N stands for the total number of degrees of freedom defining $\mathbb{H}^{\boldsymbol{\sigma}}_{h,0} \times \mathbf{H}^{\mathbf{u}}_{h,0} \times \Psi^{\varphi}_h \times Q_h \times \mathbb{R}$ associated to the system (3.3), or $\mathbb{H}^{\boldsymbol{\sigma}}_{h,N} \times \mathbf{H}^{\mathbf{u}}_{h,0} \times \Psi^{\varphi}_h \times Q_h$ for the system (4.5). We denote the individual errors by

$$\mathtt{e}(\boldsymbol{\sigma}^{\mathrm{d}}) := \|\boldsymbol{\sigma}^{\mathrm{d}} - \boldsymbol{\sigma}^{\mathrm{d}}_h\|_{0,\Omega}\,, \quad \mathtt{e}(\mathbf{u}) := \|\mathbf{u} - \mathbf{u}_h\|_{0,\Omega}\,, \quad \mathtt{e}(p) := \|p - p_h\|_{0,\Omega}\,,$$

$$\mathtt{e}(\varphi) := |\varphi_h|_h\,, \quad \mathtt{e}(\mathbf{f}) := \|\mathbf{f} - \mathbf{P}_h(\mathbf{f})\|_{0,\Omega}$$

where p is the exact pressure that can be recovered through the identity $p = -\frac{\nu}{d}\,\mathrm{tr}\,(\boldsymbol{\sigma})$ and the approximate pressure p_h is computed through the postprocessing formula $p_h = -\frac{\nu}{d}\mathrm{tr}\,(\boldsymbol{\sigma}_h)$.

In addition, we let $r(\%)$ be the experimental rate of convergence given by

$$r(\%) := \frac{\log(\mathtt{e}(\%)/\mathtt{e}'(\%))}{\log(h/h')},$$

where $\mathtt{e}(\%)$ is any of the errors defined above and h and h' are two consecutive meshsizes with errors $\mathtt{e}$ and $\mathtt{e}'$.

Example 1: Rates of convergence

The first example focuses on illustrating the performance of the two dimensional mixed finite element scheme under a quasi-uniform refinement, by considering manufactured exact solution $(\mathbf{u}, p)$ in the domain $\Omega = (0,1)^2$ given by

$$\mathbf{u}(x_1, x_2) = \begin{pmatrix} \pi \exp(x_1)\cos(\pi x_2) \\ \\ -\exp(x_1)\sin(\pi x_2) \end{pmatrix}, \quad p(x_1, x_2) = x_1^3 + x_2^3 - 0.5\,.$$

In this case,

$$\mathbf{f} = \begin{pmatrix} 3x_1^2 + \nu\pi\exp(x_1)\cos(\pi x_2)(\pi^2 - 1) \\ \\ 3x_2^2 - \nu\exp(x_1)\sin(\pi 2x_2)(\pi^2 - 1) \end{pmatrix}.$$

In Table 5.1, we summarize the convergence history for a sequence of quasi-uniform triangulations, considering the viscosity $\nu = 1$ and ν =1.0E-3. We see there that the rate of convergence provided by Theorem 3.4 is attained by all the unknowns. We emphasize that, when comparing the errors obtained for $\nu = 1$ and ν=1.0E-3, the numerical results indicate that these errors are not amplified by the factor ν^{-1}. In addition, the l^∞–norm of $\mathrm{div}\,\mathbf{u}_h$ in each mesh is close to 0 which shows that this method is mass conserving. From the columns corresponding to $\|\mathbf{div}\,\boldsymbol{\sigma}_h + \nu^{-1}\mathbf{f}\|_{0,\Omega}$ and $\mathtt{e}(\mathbf{f})$, we observe that for $\nu = 1.0$, both columns exhibit similar magnitudes. In contrast, for ν=1.0E-3, the column corresponding to $\|\mathbf{div}\,\boldsymbol{\sigma}_h + \nu^{-1}\mathbf{f}\|_{0,\Omega}$ matches the column for $\mathtt{e}(\mathbf{f})$ scaled by a factor of ν^{-1}, and the convergence rate is of order 1. This numerical evidence confirms the theoretical prediction given in (3.12).

Example 2: Momentum conservation

The second example addresses the momentum conservation of the method when the datum $\mathbf{f} \in \mathbf{Q}_h$. To that end, we consider the manufactured solution $(\mathbf{u}, p)$ in the domain $\Omega = (0,1)^2$

NUMERICAL RESULTS FOR ν=1.0

N	h	$\mathsf{e}(\boldsymbol{\sigma}^{\mathrm{d}})$	$r(\boldsymbol{\sigma}^{\mathrm{d}})$	$\mathsf{e}(\mathbf{u})$	$r(\mathbf{u})$	$\mathsf{e}(p)$	$r(p)$	$\mathsf{e}(\varphi)$	$r(\varphi_h)$
409	0.372	3.941E-1	–	1.138	–	3.253E-1	–	0.765	–
1637	0.190	0.741E-1	2.483	0.487	1.261	0.557E-1	2.619	0.323	1.279
6213	0.095	0.192E-1	1.944	0.246	0.987	0.148E-1	1.909	0.160	1.017
24445	0.049	0.046E-1	2.178	0.122	1.058	0.036E-1	2.132	0.080	1.052
97129	0.024	0.012E-1	1.898	0.062	0.970	0.009E-1	1.993	0.040	0.960
391577	0.014	0.003E-1	2.581	0.031	1.268	0.002E-1	2.447	0.020	1.280

$\|\mathrm{div}\,\mathbf{u}_h\|_{l^\infty}$	$\|\mathbf{div}\,\boldsymbol{\sigma}_h + \nu^{-1}\mathbf{f}\|_{0,\Omega}$	$\mathsf{e}(\mathbf{f})$	$r(\mathbf{f})$
7.1E-15	7.500	7.531	–
5.7E-14	3.244	3.248	1.249
8.7E-14	1.662	1.662	0.966
2.3E-13	0.823	0.823	1.063
4.5E-13	0.416	0.417	0.977
9.1E-13	0.206	0.206	1.258

NUMERICAL RESULTS FOR ν=1.0E-3

N	h	$\mathsf{e}(\boldsymbol{\sigma}^{d})$	$r(\boldsymbol{\sigma}^{d})$	$\mathsf{e}(\mathbf{u})$	$r(\mathbf{u})$	$\mathsf{e}(p)$	$r(p)$	$\mathsf{e}(\varphi)$	$r(\varphi_h)$
409	0.372	6.083	–	1.148	–	1.418E-2	–	0.777	–
1637	0.190	1.276	2.320	0.488	1.261	0.300E-2	2.307	0.322	1.311
6213	0.095	0.323	1.983	0.246	0.987	0.072E-2	2.049	0.159	1.014
24445	0.049	0.078	2.139	0.122	1.058	0.017E-2	2.159	0.080	1.049
97129	0.024	0.019	1.999	0.062	0.970	0.005E-2	1.934	0.040	0.960
391577	0.014	0.005	2.526	0.031	1.268	0.001E-2	2.537	0.020	1.280

$\|\mathrm{div}\,\mathbf{u}_h\|_{l^\infty}$	$\|\mathbf{div}\,\boldsymbol{\sigma}_h + \nu^{-1}\mathbf{f}\|_{0,\Omega}$	$\mathsf{e}(\mathbf{f})$	$r(\mathbf{f})$
9.3E-15	288.009	0.288	–
2.8E-14	132.239	0.132	1.158
5.7E-14	65.772	0.065	1.008
1.7E-13	32.422	0.032	1.068
3.4E-13	16.399	0.016	0.989
9.1E-13	8.119	0.008	1.257

Table 5.1: EXAMPLE 1: Degrees of freedom, mesh sizes, errors, convergence rates, L^∞-norm of $\mathrm{div}\,\mathbf{u}_h$, L^2-norm of the discrete momentum equation, error in the projection of $\mathbf{f}$, and its convergence rate for the Galerkin scheme with $\nu = 1.0$ and $\nu = 1.0\text{E-}3$.

given by:

$$\mathbf{u}(x_1, x_2) \;=\; \begin{pmatrix} x_2^2 \\ \\ -x_1^2 \end{pmatrix}, \qquad p(x_1, x_2) \;=\; x_1 + x_2 - 1\,,$$

so that the datum $\mathbf{f}$ becomes,

$$\mathbf{f} = \begin{pmatrix} 1-2\nu \\ \\ 1+2\nu \end{pmatrix} \in \mathbf{Q}_h.$$

We run the code for viscosity values $\nu = 1.0$ and $\nu = 1.0\text{E-}3$, using a sequence of quasi-uniform triangulations.

Table 5.2 presents the l^∞-norm of $\operatorname{div} \mathbf{u}_h$ and $\mathbf{div}\, \boldsymbol{\sigma}_h + \nu^{-1}\mathbf{f}$. From these results, we observe that both quantities remain close to zero, confirming that the method is mass conservative and preserves momentum when $\mathbf{f} \in \mathbf{Q}_h$.

Furthermore, by comparing both tables, we observe that the l^∞-norm of $\mathbf{div}\, \boldsymbol{\sigma}_h + \nu^{-1}\mathbf{f}$ scales with ν^{-1}, whereas the l^∞-norm of $\operatorname{div} \mathbf{u}_h$ appears to remain unaffected by ν.

Mass and momentum conservation for ν=1.0

h	$\|\operatorname{div} \mathbf{u}_h\|_{l^\infty}$	$\|\mathbf{div}\, \boldsymbol{\sigma}_h + \nu^{-1}\mathbf{f}\|_{l^\infty}$
0.372	1.78E-15	3.55E-15
0.190	4.44E-15	1.24E-14
0.095	1.42E-14	2.84E-14
0.049	2.84E-14	1.14E-13
0.024	5.68E-14	2.27E-10
0.014	1.42E-13	4.55E-10

Mass and momentum conservation for ν=1.0E-3

h	$\|\operatorname{div} \mathbf{u}_h\|_{l^\infty}$	$\|\mathbf{div}\, \boldsymbol{\sigma}_h + \nu^{-1}\mathbf{f}\|_{l^\infty}$
0.372	1.78E-15	2.96E-12
0.190	3.55E-15	7.05E-12
0.095	1.07E-14	1.82E-11
0.049	2.84E-14	4.37E-11
0.024	5.68E-14	1.02E-10
0.014	1.26E-13	2.91E-10

Table 5.2: Example 2: Mesh sizes, L^∞-norm of $\operatorname{div} \mathbf{u}_h$ and $\mathbf{div}\, \boldsymbol{\sigma}_h + \nu^{-1}\mathbf{f}$, with $\nu = 1.0$ and $\nu = 1.0\text{E-}3$.

Example 3: Lack of pressure robustness

The third example examines the lack of pressure robustness of the method. To this end, we use the data presented in [15, Example 1.1]. Specifically, we consider the exact solutions:

$$\mathbf{u}(x_1, x_2) = \mathbf{0} \quad \text{and} \quad p(x_1, x_2) = Ra\left(x_2^3 - \frac{1}{2}x_2^2 + x_2 - \frac{7}{12}\right),$$

which results in the forcing term:

$$\mathbf{f} = \begin{pmatrix} 0 \\ \\ Ra(1 - x_2 + 3x_2^2) \end{pmatrix} \in \mathbf{Q}_h,$$

where $Ra > 0$ is a given parameter that affects only the pressure and will be assigned different values in the analysis.

In Table 5.3 we present the errors for each variable for different values of Ra. We consider a fix triangulation of size $h = 0.0244$. There, it can be appreciated that when Ra increases, all the errors increase in the same order, which confirms the aforementioned lack of pressure robustness of the method.

LACK OF PRESSURE ROBUSTNESS

Ra	$\mathsf{e}(\boldsymbol{\sigma}^d)$	$\mathsf{e}(\mathbf{u})$	$\mathsf{e}(p)$	$\mathsf{e}(\varphi)$
1.0E+0	1.593E-5	8.903E-8	2.759E-5	4.123E-8
1.0E+1	1.593E-4	8.903E-7	2.759E-4	4.123E-7
1.0E+2	1.593E-3	8.903E-6	2.759E-3	4.123E-6
1.0E+3	1.593E-2	8.903E-5	2.759E-2	4.123E-5
1.0E+4	1.593E-1	8.903E-4	2.759E-1	4.123E-4

Table 5.3: EXAMPLE 3: Errors for each variable, considering different values of Ra.

EXAMPLE 4: BACKWARD-FACING STEP FLOW

Finally, the fourth example examines mass loss in the standard backward-facing step flow test, similarly as in [3]. For this test, we consider a rectangular domain $\Omega = [0, 10] \times [0, 1]$ with a re-entrant corner at $(2, 0.5)$. The boundary Γ is partitioned into three segments: the inflow boundary Γ_{in}, the outflow boundary Γ_{out}, and the wall boundary Γ_{wall}, where $\Gamma_{wall} = \Gamma \setminus \left(\overline{\Gamma}_{in} \cup \overline{\Gamma}_{out}\right)$ (see Figure 5.1). We consider $\nu = 1.0$ and $\mathbf{f}(x_1, x_2) = \mathbf{0}$ in Ω. The boundary

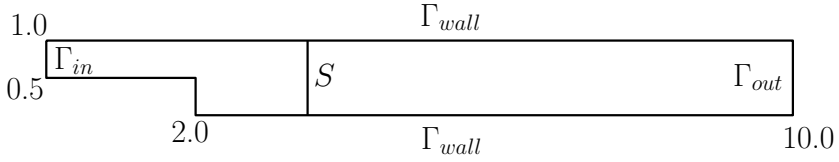

Figure 5.1: Example 4: Geometry for the backward-facing step flow test.

conditions are prescribed as follows: a parabolic inflow profile $\mathbf{u}_D(x_1, x_2) = (8(x_2 - 0.5)(1 - x_2), 0)^t$ on Γ_{in}, a no-slip condition $\mathbf{u}_D(x_1, x_2) = \mathbf{0}$ on Γ_{wall}, and, unlike [3], a *do-nothing* boundary condition is imposed on Γ_{out}, given by $\boldsymbol{\sigma}\mathbf{n} = \mathbf{0}$ on Γ_{out}.

To evaluate mass conservation in the discrete solution, we measure the total mass flow across a sequence of vertical surfaces connecting the top and bottom boundaries of the computational domain. The line labeled "S" in Figure 5.1 illustrates a representative example of such a surface for the test problem.

Since $\operatorname{div} \mathbf{u} = 0$ in Ω, from the divergence theorem it follows that

$$\int_{\Gamma_{in}} \mathbf{u} \cdot \mathbf{n} = \int_S \mathbf{u} \cdot \mathbf{n}_S,$$

for any S connecting the top and bottom walls of the domain. Then, suggested by the above, in what follows, mass conservation in the discrete solution will be quantified by the percentage

mass loss across the surface S, defined as

$$\%m_{loss} := 100 \frac{\left| \int_{\Gamma_{in}} \mathbf{u}_h \cdot \mathbf{n} - \int_S \mathbf{u}_h \cdot \mathbf{n}_S \right|}{\left| \int_{\Gamma_{in}} \mathbf{u}_h \cdot \mathbf{n} \right|}. \tag{5.1}$$

We compare the mass loss in (4.5) against the standard discrete pseudostress-based scheme for (4.1), formulated as follows: find $\boldsymbol{\sigma}_h \in \mathbb{H}^{\boldsymbol{\sigma}}_{h,N}$ and $\mathbf{u}_h \in \mathbf{Q}_h$ such that

$$\begin{aligned} (\boldsymbol{\sigma}_h^{\mathrm{d}}, \boldsymbol{\tau}_h^{\mathrm{d}})_\Omega + (\mathbf{u}_h, \mathbf{div}\, \boldsymbol{\tau}_h)_\Omega &= \langle \boldsymbol{\tau}_h \mathbf{n}, \mathbf{u}_D \rangle_{\Gamma_D}, \quad \forall \boldsymbol{\tau}_h \in \mathbb{H}^{\boldsymbol{\sigma}}_{h,N}, \\ (\mathbf{v}_h, \mathbf{div}\, \boldsymbol{\sigma}_h)_\Omega &= -\frac{1}{\nu}(\mathbf{f}, \mathbf{v}_h)_\Omega, \quad \forall \mathbf{v}_h \in \mathbf{Q}_h, \end{aligned} \tag{5.2}$$

with $\Gamma_N = \Gamma_{out}$ and $\Gamma_D = \Gamma \setminus \Gamma_{out}$.

We use a computational grid consisting of 120.926 triangles with a mesh size of $h = 0.0212$, leading to a total of $N = 1.214.540$ degrees of freedom for the mass-conservative scheme (4.5) and $N = 1.274.123$ for (5.2). Notice that, despite the fact that (4.5) involves three unknowns while (5.2) considers only two, the former is slightly less computationally expensive than the latter.

The results of our study are summarized in Figure 5.2, where we compare the mass losses obtained using formulation (4.5) with those from (5.2), considering 100 lines S equally distributed in Ω. The figure clearly demonstrates a significant improvement in mass conservation, as quantified by the percent mass loss formula (5.1). Specifically, in (4.5), the maximum mass loss remains below 0.1%, whereas in (5.2), it exceeds 1.0%.

In Figure 5.3, we present the pressure distribution (top panel), velocity magnitude (center panel), and streamlines (bottom panel) obtained using the scheme (4.5). The results exhibit the expected behavior: high pressure near the inlet, a characteristic parabolic velocity profile throughout the full length of the domain with higher velocity near the inlet, and the formation of the expected vortex below the re-entrant corner.

References

[1] A. Alonso-Rodríguez, J. Camaño, Riccardo Ghiloni and Alberto Valli. *Graphs, spanning trees and divergence-free finite elements in domains of general topology.* IMA J. Numer. Anal. 37 (2017), no. 4, 1986–2003.

[2] D.N. Arnold and R.S. Falk. *A uniformly accurate finite element method for the Reissner–Mindlin plate.* SIAM J. Numer. Anal. 26 (1989), no. 6, 1276–1290.

[3] P. Bochev, J. Lai and L. Olson. *A locally conservative, discontinuous least-squares finite element method for the Stokes equations.* Internat. J. Numer. Methods Fluids 68 (2012), no. 6, 782–804.

[4] D. Boffi, F. Brezzi and M. Fortin. *Mixed Finite Element Methods and Applications.* Springer Series in Computational Mathematics, Springer, Heidelberg, vol. 44, 2013.

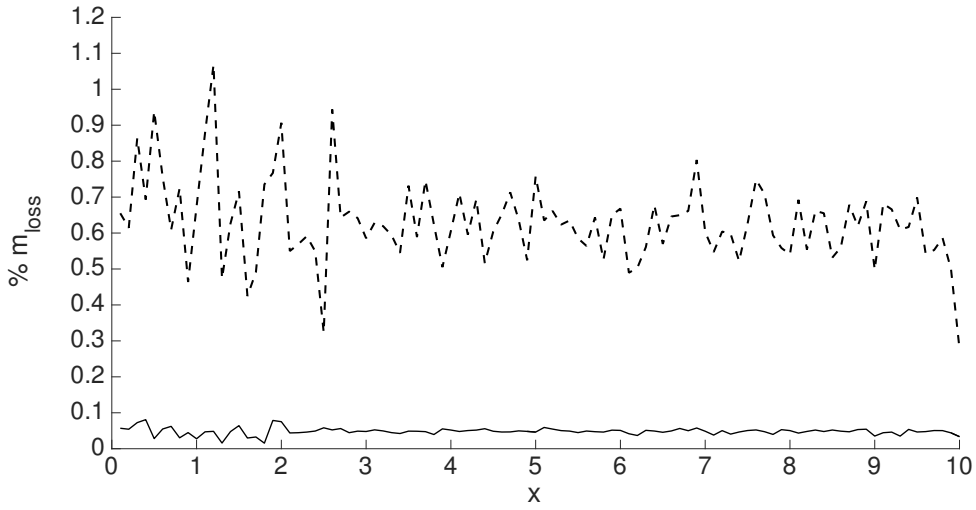

Figure 5.2: Example 4: Comparison of mass losses in (4.5) and (5.2) using 100 equally spaced lines in Ω.

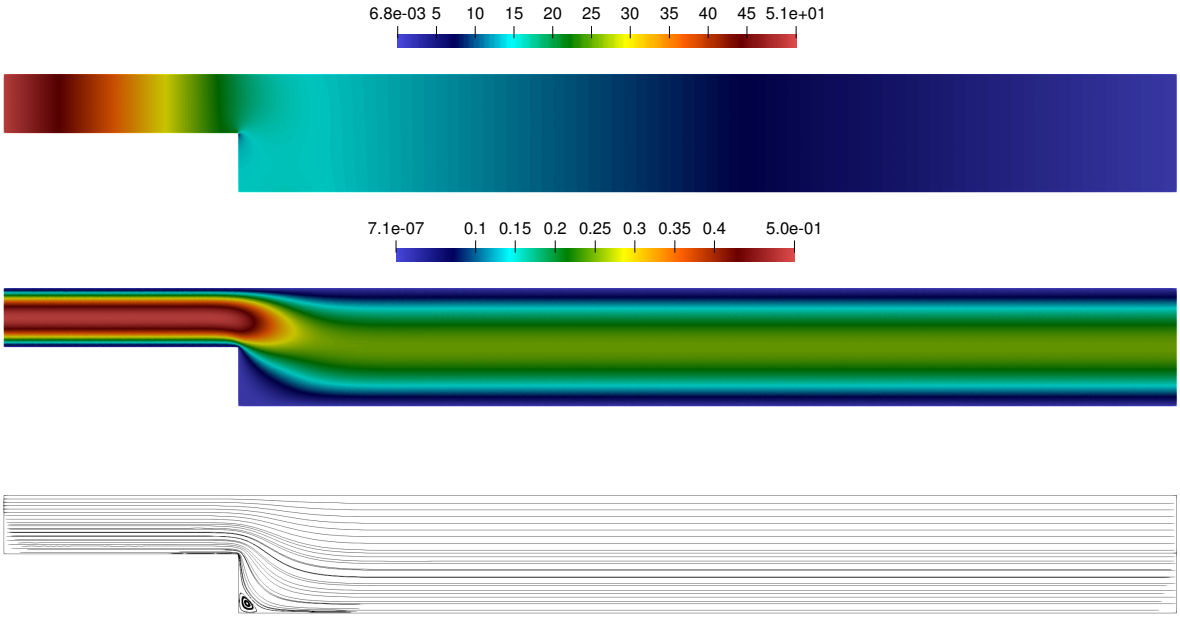

Figure 5.3: Example 4: Pressure (top panel), velocity magnitude (center panel) and streamlines (bottom panel).

[5] Z. Cai, Ch. Tong, P.S. Vassilevski and Ch. Wang. *Mixed finite element methods for incompressible flow: stationary Stokes equations*. Numer. Methods Partial Differential Equations 26 (2010), no. 4, 957–978.

[6] J. Camaño and R. Oyarzúa. *A conforming and mass conservative pseudostress-based mixed finite element method for Stokes*. Preprint 2023-15, Centro de Investigacin en Ingeniera Matemtica (CI2MA), UdeC.

[7] M. Crouzex and P.-A. Raviart. *Conforming and nonconforming finite element methods for solving the stationary Stokes equations I.* R.A.I.R.O., 7 (1973), no. R–3, 33–75.

[8] T.A. Davis. *Algorithm 832: UMFPACK V4.3 - an unsymmetric-pattern multifrontal method*. ACM Trans. Math. Software 30 (2004), no. 2, 196–199.

[9] G.N. Gatica. A Simple Introduction to the Mixed Finite Element Method. Theory and Applications, Springer Briefs in Mathematics, Springer, Cham Heidelberg New York Dordrecht London, 2014.

[10] G.N. Gatica, A. Márquez and M. Sánchez. *Analysis of a velocity-pressure-pseudostress formulation for incompressible flow.* Comput. Methods Appl. Mech. Engrg. 199 (2010), no. 17-20, 1064–1079.

[11] G.N. Gatica, A. Márquez and M. Sánchez. *Pseudostress-based mixed finite element methods for the Stokes problem in R^n with Dirichlet boundary conditions. I: A priori error analysis*. Commun. Comput. Phys. 12 (2012), no. 1, 109–134.

[12] P. Grisvard. Elliptic Problems in Nonsmooth Domains. Classics in Applied Mathematics, 69. Society for Industrial and Applied Mathematics (SIAM), Philadelphia, PA, 2011.

[13] F. Hecht. *New development in FreeFem++*. J. Numer. Math. 20 (2012), no. 3–4, 251–266.

[14] V. John. Finite element methods for incompressible flow problems. Springer Series in Computational Mathematics, 51. Springer, Cham, 2016. xiii+812 pp.

[15] V. John, A. Linke, C. Merdon, M. Neilan, and L.G. Rebholz. *On the divergence constraint in mixed finite element methods for incompressible flows*. SIAM Rev. 59 (2017), no. 3, 492–544.

[16] P.L. Lederer and C. Merdon. *Guaranteed upper bounds for the velocity error of pressure-robust Stokes discretisations* J. Numer. Math. 30 (2022), no. 4, 267–294.

[17] P. Monk. *A mixed method for approximating Maxwells equations*. SIAM J. Numer. Anal. 28 (1991), no. 6, 1610–1634.

Centro de Investigación en Ingeniería Matemática (CI^{2}MA)

PRE-PUBLICACIONES 2024 - 2025

2024-22 Anahi Gajardo, Victor H. Lutfalla, Michaël Rao: *Ants on the highway*

2024-23 Julio Aracena, Luis Cabrera-Crot, Adrien Richard, Lilian Salinas: *Dynamically equivalent disjunctive networks*

2024-24 Julio Aracena, Raúl Astete-Elguin: *K-independent boolean networks*

2024-25 Sergio Carrasco, Sergio Caucao, Gabriel N. Gatica: *A twofold perturbed saddle point-based fully mixed finite element method for the coupled Brinkman Forchheimer Darcy problem*

2024-26 Juan Barajas-Calonge, Raimund Bürger, Pep Mulet, Luis M. Villada: *Invariant-region-preserving central WENO schemes for one-dimensional multispecies kinematic flow models*

2024-27 Raimund Bürger, Claudio Muñoz, Sebastián Tapia: *Interaction of jamitons in second-order macroscopic traffic models*

2025-01 Boumediene Chentouf, Sabeur Mansouri, Mauricio Sepúlveda, Rodrigo Véjar: *Theoretical and numerical results for the exponential stability of the rotating disk-beam system with a boundary infinite memory of type angular velocity*

2025-02 Julio Aracena, Arturo Zapata-Cortés: *Hamiltonian dynamics of boolean networks*

2025-03 Raimund Bürger, Andrés Guerra, Carlos A. Vega: *An entropy stable and well-balanced scheme for an augmented blood flow model with variable geometrical and mechanical properties*

2025-04 Alonso Bustos, Sergio Caucao, Gabriel N. Gatica, Benjamín Venegas: *New fully mixed finite element methods for the coupled convective Brinkman-Forchheimer and nonlinear transport equations*

2025-05 Fahim Aslam, Zayd Hajjej, Jianghao Hao, Mauricio Sepúlveda: *Global Existence and Asymptotic Profile of an Infinite Memory Logarithmic Wave Equation with Fractional Derivative and Strong Damping*

2025-06 Jessika Camaño, Ricardo Oyarzúa, Katherine Rojo: *A momentum and mass conservative pseudostress-based mixed finite element method for the Stokes problem*

Para obtener copias de las Pre-Publicaciones, escribir o llamar a: Director, Centro de Investigación en Ingeniería Matemática, Universidad de Concepción, Casilla 160-C, Concepción, Chile, Tel.: 41-2661324, o bien, visitar la página web del centro: `http://www.ci2ma.udec.cl`







Centro de Investigación en
Ingeniería Matemática (CI²MA)
Universidad de Concepción

Casilla 160-C, Concepción, Chile
Tel.: 56-41-2661324/2661554/2661316
http://www.ci2ma.udec.cl